
MM-Prompt: Cross-Modal Prompt Tuning for Continual Visual Question Answering

Xu Li¹ Fan Lyu^{2*}

¹Khoury College of Computer Sciences, Northeastern University

²New Laboratory of Pattern Recognition, Institute of Automation, Chinese Academy of Sciences

li.xu2@northeastern.edu fan.lyu@cripac.ia.ac.cn

Abstract

Continual Visual Question Answering (CVQA) based on pre-trained models (PTMs) has achieved promising progress by leveraging prompt tuning to enable continual multi-modal learning. However, most existing methods adopt cross-modal prompt isolation, constructing visual and textual prompts separately, which exacerbates modality imbalance and leads to degraded performance over time. To tackle this issue, we propose MM-Prompt, a novel framework incorporating cross-modal prompt query and cross-modal prompt recovery. The former enables balanced prompt selection by incorporating cross-modal signals during query formation, while the latter promotes joint prompt reconstruction through iterative cross-modal interactions, guided by an alignment loss to prevent representational drift. Extensive experiments show that MM-Prompt surpasses prior approaches in accuracy and knowledge retention, while maintaining balanced modality engagement throughout continual learning. Our code is available at <https://github.com/xli04/CVQA>.

1 Introduction

Pre-trained models (PTMs) have achieved considerable success in Visual Question Answering (VQA) [1–3], a traditional multi-modal task that generates answers to questions based on relevant images. Recently, researchers further extended PTMs to Continual VQA (CVQA) [4–9], where new content emerges over time, with approaches developed to address the challenge of catastrophic forgetting. **Prompt tuning**, a PTM-based method proven effective in CL [10–16], which first selects prompts based on input representations via similarity, then injects the selected prompts into encoders to guide learning. This approach has shown good performance in CVQA [4, 6, 8, 9]. For example, [6] introduces a fusion-prompt pool to complement visual and textual prompts, [8] replays scene-graph prompts to enhance generalization, and [9] applies K-means clustering to define modality-aware prompt centers.

However, most prompt-based CVQA methods adopt a *cross-modal prompt isolation* approach, constructing and utilizing visual and textual prompts independently without complementary knowledge understanding [4, 6, 8–13, 17]. As illustrated in Fig. 1a, these methods select and process prompts separately for vision and language, without mechanisms for cross-modal interaction. This isolated approach is suboptimal for CVQA, where language features naturally tend to be dominant [18]. Injecting such modality-isolated prompts amplifies the existing imbalance by providing the model with additional information from its already-preferred modality, diminishing the ability to integrate cross-modal representations. As a result, performance degrades as the model increasingly relies on one modality.

*Corresponding author.

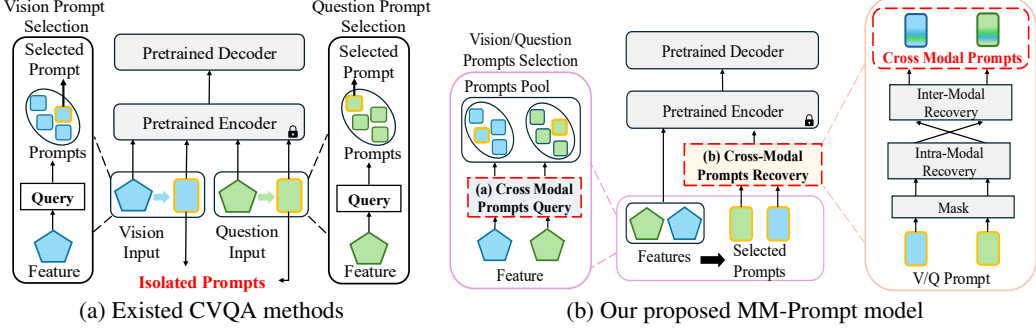


Figure 1: Comparison between traditional prompt-based CVQA approaches and MM-Prompt. Previous methods rely on isolated prompt pools, letting modality-isolated biases accumulate, whereas MM-Prompt introduces explicit cross-modal interactions that yield more balanced predictions over sequential tasks.

To avoid cross-modal prompt isolation and disrupt the error accumulation of modality imbalance in the two stages, i.e., prompt query and injection, we propose MM-Prompt, as shown in Fig. 1b. MM-Prompt consists of two key components, including cross-modal prompt query and cross-modal prompt recovery. First, the *cross-modal prompt query* module enhances prompt selection by mixing information from the opposite modality into each query prior to retrieval, enabling more balanced and context-aware selection. Second, the *cross-modal prompt recovery* module jointly masks and reconstructs prompts through progressively enriched cross-modal interactions, effectively embedding fused information into the prompt space before the injection stage. Alignment losses are applied to prevent representational drift. Together, these components promote balanced modality utilization, enhance accuracy, and reduce forgetting. Experimental results show that MM-Prompt not only surpasses prior prompt-based methods in performance and retention but also sustains more balanced modality engagement across sequential tasks, effectively addressing the performance degradation caused by modality-isolated prompts that underlies prior failures. Our contributions are three-fold:

- (1) We show that the cross-modal prompt isolation approach adopted by existing prompt-based CVQA methods progressively amplifies modality imbalance, undermines multimodal reasoning capabilities, and ultimately degrades performance.
- (2) We propose Cross-Modal Prompts Query, a mechanism that enriches modality-specific features with complementary information before prompt selection, preventing prompts from reinforcing single-modality specialization
- (3) We develop Cross-Modal Prompts Recovery, a masking then hierarchical recovery approach that enforces interactions between modalities and common knowledge understanding between modalities through structured cross-modal pathways

2 Related Work

Continual Visual Question Answering. VQA combines visual and language representations to answer questions about images [19, 20], while continual learning builds models that preserve previous knowledge when learning new information [21]. CVQA integrates these approaches by sequentially updating models on new image-question-answer tasks [4, 6, 8–13, 17]. Approaches to address forgetting in CL include regularization-based[22, 23], architecture-based[24, 25], replay-based[26, 27], and prompt-based methods [4, 6, 8–13, 17]. While the first three typically require full fine-tuning, prompt-based methods keep backbones frozen and only update lightweight prompts, offering better efficiency. L2P [11], which selects prompts based on query similarity, Dual Prompt [10], which uses general and expert prompts at different layers and CODA [12], which injects weighted combinations of prompt components. Despite their success in general continual learning, prompt methods struggle with CVQA’s unique challenges. CVQA suffers from catastrophic forgetting [28] and modality imbalance [29, 30]. Existing prompt methods select and inject prompts in a modality-specific pattern, providing more information to the model’s preferred modality, typically language [29], which reinforces modality bias and hinders cross-modal integration. As a result, the visual features are further marginalized, and the model’s performance degrades over time.

Pre-trained Models with Prompt Tuning in CL. Pretrained models contain rich, generalizable knowledge for downstream tasks [31–35]. Among CL approaches, prompt-based methods [4, 6, 8–13, 17, 36] are the most ideal for pretrained models as they preserve capabilities by keeping back-

bones frozen. While most prompt methods were developed for unimodal settings [10–12], several recent works explore multimodal prompt learning [4, 6, 8, 9, 17]. [6] introduced fusion prompt pools with interaction matrices to bridge modalities. [8] employs scene graphs as symbolic representations to encourage generalized learning across modalities. [9] uses a two-stage process with K-means clustering to establish modality-specific centers before merging them. Despite these advances, we argue these approaches remain suboptimal for CVQA. As learning progresses, modality-specific differences accumulate within prompts without explicit balancing mechanisms. The selected prompts inevitably carry modality-imbalanced information, which can further exacerbate modality disparity and impair cross-modal integration when injected into the model.

Cross Modal Interaction A number of vision–language models have explored explicit cross-modal alignment and fusion strategies in static, single-task settings [37–39]. Attention Bottlenecks [37] align modalities by routing inter-modal information through a small set of shared bottleneck tokens, with early independent processing followed by mid-level fusion. DIFNet [38] aligns complementary visual streams using Iterative Independent Layer Normalization, preserving modality-specific cues via shared weights and separate normalization. MIA [39] uses mutual iterative attention, alternately attending between visual regions and textual concepts before fusing the aligned features. While effective for joint learning, these designs are suboptimal for Continual VQA. Their fusion mechanisms require continual fine-tuning, which overwrites knowledge from previous tasks and makes them highly prone to catastrophic forgetting. In addition, their static fusion strategies lack the adaptability needed to mitigate the modality imbalance that often emerges and accumulated across sequential tasks in CVQA.

3 Proposed Method

3.1 Problem Formulation

Following [4], we formulate CVQA as T sequential incremental tasks corresponding to the training data $\{\mathcal{D}_1, \dots, \mathcal{D}_T\}$. For task t , $\mathcal{D}_t = \{(x_i^Q, x_i^V, y_i)\}_{i=1}^{n_t}$, where x_i^V represents input image, x_i^Q denotes questions about this image, and y_i represents the corresponding true label. During training, models must learn new visual concepts without revisiting prior data, and retain performance on all previous tasks. In this paper, we consider three incremental learning settings: Question Increment (QI), Class Increment (CI), and Dual Increment (DI) [4]. In QI, each task introduces new question types while sharing all object classes across tasks. In CI, each task adds new object classes with shared all question types. DI combines both, in which each task has S subtasks sharing the same visual classes but introducing new question types, while visual classes differ between tasks.

Existing prompt-based methods [4, 6, 9–13, 17] employ prompt pools, i.e., sets of learnable prompts with associated keys, to store task-specific knowledge. Prompts are used in two stages: first select via query-key matching with input-derived queries and then inject into encoder layers to guide representation learning. However, existing approaches follow a cross-modal prompt isolation strategy, relying on unimodal features for prompt selection and injection, without cross-modal interaction. This reinforces alignment with modality-specific feature distributions, amplifies the dominant modality bias, and hinders the integration of complementary information. To overcome this, we propose MM-Prompt, which introduces two core components: (1) **cross-modal prompt query**, enabling prompt selection guided by fused modality signals, and (2) **cross-modal prompt recovery**, facilitating explicit information exchange across modalities. These components are detailed in Fig. 2.

3.2 Cross-Modal Prompt Query

In CVQA, vision and language offer complementary representations that benefit from joint modeling [19]. Inspired by this, we design a cross-modal querying mechanism that enables each modality to attend to prompts using information from the other. Specifically, we employ an attention (A) module to infuse visual context into question-side queries and linguistic context into image-side queries. For each modality, we maintain a prompt pool consisting of prompts $\mathbf{p} \in \mathcal{P}$ and corresponding keys $\mathbf{k} \in \mathcal{K}$, where \mathcal{P} and \mathcal{K} denote the sets of prompts and keys, respectively, with $\mathbf{p} \in \mathbb{R}^d$ and $\mathbf{k} \in \mathbb{R}^d$. Let $\mathbf{F}^Q \in \mathbb{R}^{l_Q \times d}$ and $\mathbf{F}^V \in \mathbb{R}^{l_V \times d}$ denote the question and vision features extracted from the x^Q, x^V , from which we derive the cross-modal queries $\mathbf{q} \in \mathbb{R}^d$ with $\mathbf{w} \in \mathbb{R}^d$:

$$\mathbf{q}^Q = \mathbf{w}^Q \odot \Phi(\mathbf{A}_{\text{query}}^Q(\mathbf{F}^Q, \mathbf{F}^V, \mathbf{F}^V) + \mathbf{F}^Q), \quad \mathbf{q}^V = \mathbf{w}^V \odot \Phi(\mathbf{A}_{\text{query}}^V(\mathbf{F}^V, \mathbf{F}^Q, \mathbf{F}^Q) + \mathbf{F}^V), \quad (1)$$

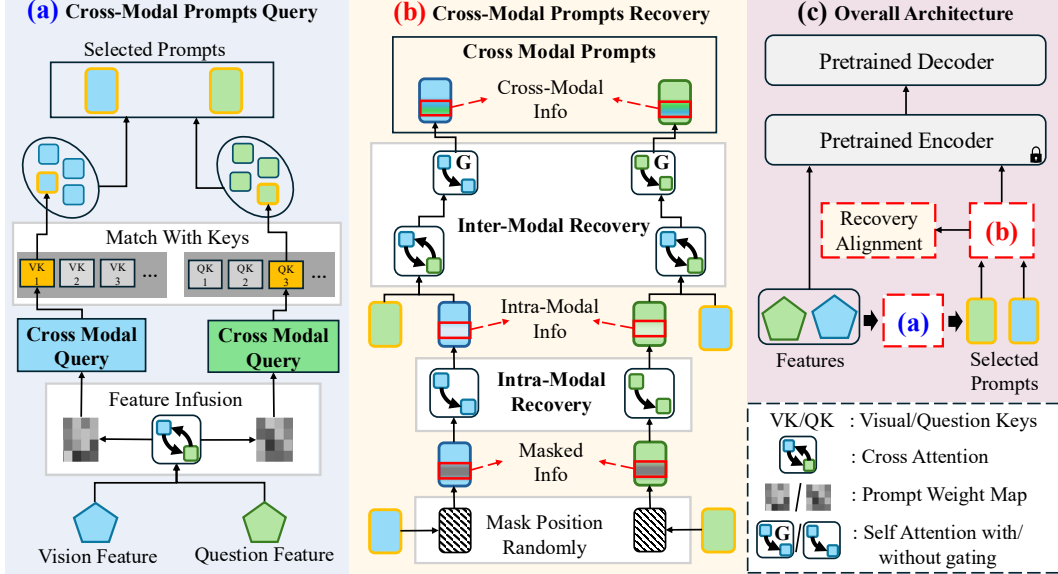


Figure 2: Detailed MM-Prompt Components for (a) Cross-Modal Prompts Query and (b) Cross-Modal Prompts Recovery from the overall architecture for MM-Prompt. Cross-modal prompts query illustrates our approach where visual (VF) and question (QF) features undergo cross-modal interaction before key matching, creating enriched queries that influence prompt selection across modalities. Cross-modal prompts recovery shows our hierarchical process: identical masks are applied to both modality prompts, followed by intra-modality recovery and inter-modality recovery. This design creates balanced integration pathways that prevent the modality isolation problem in existing prompt-based approaches.

where Φ denotes a pooling operation on the feature dimension. To enable cross-modal integration while preserving modality-specific identity, we enhance the query computation in Eq. (1) with two key components. First, the residual term ($+F^Q/F^V$) retains original modality features during fusion, preventing dilution by cross-modal signals. Second, the weight modulation terms w^Q and w^V , initialized uniformly and jointly optimized, adaptively control each feature dimension’s contribution, emphasizing informative components and suppressing noise. Together, these mechanisms ensure that the enriched queries q^Q and q^V integrate complementary cross-modal information without compromising modality fidelity, mitigating uni-modal bias and enabling balanced prompt selection.

Given the enriched queries, we first retrieve the indices for the top- k most similar prompts:

$$\mathcal{I}^M \leftarrow \text{Top-}k \left(\text{sort}(\cos(\mathbf{q}^M, \mathbf{k}^M)) \right), \quad k^M \in \mathcal{K}^M, \quad M \in \{Q, V\}, \quad (2)$$

After getting the indices, instead of relying on the top-1 prompt, which may overfit to limited patterns, we compute a weighted aggregation to construct more robust cross-modal representations $\tilde{\mathbf{p}} \in \mathbb{R}^d$. \mathbf{p}_i denotes the prompts at i th indices, the weight a_i reflects the relevance score:

$$\tilde{\mathbf{p}}^M = \sum_{i \in \mathcal{I}^M} a_i \mathbf{p}_i^M, \quad \text{where} \quad a_i = \frac{\exp(\cos(\mathbf{q}^M, \mathbf{k}_i^M))}{\sum_{j \in \mathcal{I}^M} \exp(\cos(\mathbf{q}^M, \mathbf{k}_j^M))}, \quad M \in \{Q, V\}. \quad (3)$$

By leveraging cross-modal queries, the similarity-based weighting favors prompts aligned with joint modality semantics rather than uni-modal features. This design promotes the selection of complementary cross-modal cues, effectively mitigating modality bias at the selection stage.

3.3 Cross-Modal Prompts Recovery

Existing methods inject prompts directly into encoder layers without further cross-modal interaction, overlooking the integration of complementary knowledge between modalities. This isolated injection worsens modality imbalance by supplying additional modality-specific cues, further biasing the model toward its dominant modality and impairing overall performance. To mitigate this, we propose a cross-modal recovery mechanism, which can be seen in Fig. 2(b).

Cross-Modal Masking for Alignment and Dependency. To induce structured interdependence between modalities and encourage explicit cross-modal reasoning, we introduce a shared masking strategy inspired by advances in masked representation learning [40, 41]. Specifically, we apply

identical binary masks to both visual and textual prompt sets, thereby creating aligned missing regions across modalities. These masked regions will be reconstructed using complementary information from the other modality, compelling the model to perform genuine cross-modal integration rather than relying on modality-specific priors.

As shown at the bottom of Fig. 2(b), we generate a binary mask $\mathbf{b} \in \mathbb{R}^d$, where each entry is independently set to 0 with probability δ :

$$\hat{\mathbf{p}}^M = (1 - \mathbf{b}) \odot \tilde{\mathbf{p}}^M, \quad M \in \{Q, V\}. \quad (4)$$

This aligned masking not only enforces balanced modality reliance but also establishes a foundation for hierarchical recovery. Specifically, we leverage the masked prompts in two stages: first, intra-modal recovery restores missing content using internal modality cues, followed by inter-modal recovery, which refines representations through cross-modal interactions. This two-step reconstruction enables progressive integration of modality-specific and complementary information, facilitating deeper cross-modal understanding.

Intra-Modal Prompt Recovery. Building on the structured masking, we initiate recovery with a modality-preserving strategy to prevent premature dominance by either modality. Direct cross-modal reconstruction risks overwriting modality-specific patterns or introducing biased alignment. Instead, we adopt an intra-modal recovery phase that reconstructs masked prompts using internal context, augmented with subtle cross-modal signals to establish initial cross-modality awareness. We incorporate a self-attention module $A(\cdot)$ to reconstruct masked tokens based primarily on surrounding context, while a light cross-modal term introduces influence from the opposite modality through a learnable matrix $\mathbf{w}_{\text{res}} \in \mathbb{R}^d$ initialized with very small values:

$$\mathbf{p}_{\text{intra}}^Q = A_{\text{intra}}^Q(\hat{\mathbf{p}}^Q) + \mathbf{w}_{\text{res}}^Q \odot \tilde{\mathbf{p}}^V, \quad \mathbf{p}_{\text{intra}}^V = A_{\text{intra}}^V(\hat{\mathbf{p}}^V) + \mathbf{w}_{\text{res}}^V \odot \tilde{\mathbf{p}}^Q. \quad (5)$$

To ensure fidelity and avoid representational collapse, we introduce a dual-objective loss:

$$\mathcal{L}_{\text{intra}} = \sum_{M \in \{Q, V\}} \|\mathbf{p}_{\text{intra}}^M - \tilde{\mathbf{p}}^M\|_2^2 + \|\mathbf{w}_{\text{res}}^Q(\mathbf{w}_{\text{res}}^Q)^T - \mathbf{I}\|_F^2 + \|\mathbf{w}_{\text{res}}^V(\mathbf{w}_{\text{res}}^V)^T - \mathbf{I}\|_F^2, \quad (6)$$

where the $\|\cdot\|_F$ represents the Frobenius norm and \mathbf{I} is an identity matrix. First term preserves the modality-specific information by keeping the recovered prompt close to the original selected prompt, while second and third term enforce orthogonality on the residual weights to limit redundant or overly correlated dimensions [42]. By minimizing this loss, the intra-modal recovery establishes a foundation that preserves essential modality-specific patterns while introducing initial cross-modal awareness, creating balanced representations that serve as the basis for deeper integration. However, it still remains insufficient for modeling richer interactions that require explicit cross-modality reasoning. To address this, we introduce a dedicated inter-modal prompt recovery mechanism that operates on the recovered representations to achieve deeper integration and complete the cross-modal reconstruction process.

Inter-Modal Prompt Recovery. Building upon the intra-modal recovery foundation, we next introduce explicit inter-modal integration to enable fine-grained cross-modal reasoning. To this end, we apply attention modules across modalities, allowing each modality’s prompts to selectively incorporate complementary features from the other. Residual connections ensure preservation of core modality-specific characteristics during this integration:

$$\mathbf{p}_{\text{inter}}^Q = A_{\text{inter}}^Q(\mathbf{p}_{\text{intra}}^Q, \tilde{\mathbf{p}}^V, \tilde{\mathbf{p}}^V) + \mathbf{p}_{\text{intra}}^Q, \quad \mathbf{p}_{\text{inter}}^V = A_{\text{inter}}^V(\mathbf{p}_{\text{intra}}^V, \tilde{\mathbf{p}}^Q, \tilde{\mathbf{p}}^Q) + \mathbf{p}_{\text{intra}}^V. \quad (7)$$

Eq. (7) completes coarse-level inter-modal fusion, enabling the model to capture salient cross-modal signals. However, MHA may miss fine-grained or subtle cues critical for downstream reasoning. To address this, we incorporate an additional attention module with twice feed-forward dimension capacity for refinement, but apply it selectively through a learnable gating mechanism that determines where further integration is beneficial:

$$\mathbf{p}_{\text{final}}^Q = (1 - \mathbf{g}^Q) \cdot \mathbf{p}_{\text{inter}}^Q + \mathbf{g}^Q \cdot A_{\text{gate}}^Q(\mathbf{p}_{\text{inter}}^Q), \quad \mathbf{p}_{\text{final}}^V = (1 - \mathbf{g}^V) \cdot \mathbf{p}_{\text{inter}}^V + \mathbf{g}^V \cdot A_{\text{gate}}^V(\mathbf{p}_{\text{inter}}^V), \quad (8)$$

where the gating mechanism calculates region-specific enhancement weights between 0 to 1:

$$\mathbf{g}^Q = \text{Sigmoid} \left(\mathbf{w}_g^Q \cdot \text{ReLU} \left([\mathbf{p}_{\text{inter}}^Q; \tilde{\mathbf{p}}^V] \right) \right), \quad \mathbf{g}^V = \text{Sigmoid} \left(\mathbf{w}_g^V \cdot \text{ReLU} \left([\mathbf{p}_{\text{inter}}^V; \tilde{\mathbf{p}}^Q] \right) \right), \quad (9)$$

where $[\cdot; \cdot]$ represents the concatenation along the feature dimension and $\mathbf{w}_g \in \mathbb{R}^d$ is a learnable weight matrix that allows the model to adaptively select the areas for enhancement. This design ensures that additional refinement is only performed when supported by strong cross-modal evidence, thus avoiding unnecessary interference and preserving representational sparsity.

To improve inter-modal consistency, we introduce a cross-modal alignment loss that enforces semantic agreement between dual perspectives—how question features are contextualized by vision and vice versa (Numerator):

$$\mathcal{L}_{\text{inter}} = 1 - \frac{\mathbf{A}_{\text{loss}}^Q(\mathbf{p}_{\text{final}}^Q, \tilde{\mathbf{p}}^V, \tilde{\mathbf{p}}^V) \cdot \mathbf{A}_{\text{loss}}^V(\mathbf{p}_{\text{final}}^V, \tilde{\mathbf{p}}^Q, \tilde{\mathbf{p}}^Q)}{\|\mathbf{A}_{\text{loss}}^Q(\mathbf{p}_{\text{final}}^Q, \tilde{\mathbf{p}}^V, \tilde{\mathbf{p}}^V)\|_2 \cdot \|\mathbf{A}_{\text{loss}}^V(\mathbf{p}_{\text{final}}^V, \tilde{\mathbf{p}}^Q, \tilde{\mathbf{p}}^Q)\|_2}, \quad (10)$$

where Denominator normalizes both scores to focus on directional agreement rather than magnitude. By minimizing this loss, we encourage bidirectional semantic coherence and prevent representational drift as the model adapts to new tasks.

In summary, inter-modal recovery completes the masked prompt reconstruction pipeline by explicitly integrating cross-modal cues through attention, selective enhancement, and alignment. This phase ensures that final prompt representations are not only modality-aware but also deeply fused, facilitating robust and balanced multimodal reasoning.

3.4 Training Objective

Finally, these cross-modal prompts are then injected into the frozen pretrained encoder layers. This entire process is trained end-to-end with a multi-component objective:

$$\mathcal{L}_{\text{total}} = \mathcal{L}_{\text{CE}} + \mathcal{L}_{\text{qk-align}} + \alpha \mathcal{L}_{\text{inter}} + \beta \mathcal{L}_{\text{intra}}, \quad (11)$$

where \mathcal{L}_{CE} is the cross entropy loss that optimizes task performance. $\mathcal{L}_{\text{qk-align}} = \sum_{i \in \mathcal{I}^M}^{M \in \{Q, V\}} (1 - \cos(\mathbf{q}^M, \mathbf{k}_i^M))$ maintains structural quality of our representations through query-key alignment [10, 11]. $\mathcal{L}_{\text{inter}}$ and $\mathcal{L}_{\text{intra}}$ ensure consistency between recovered representations during both intra-modal recovery and inter-modal recovery phases. This multi-component loss jointly optimizes for predictive accuracy, cross-modal alignment, and recovery quality, creating a balanced optimization objective that effectively enhances the quality and utility of cross-modal prompts.

As illustrated in Fig. 1, our MM-Prompt model differs fundamentally from existing CVQA approaches [4, 6, 9–13, 17] by introducing explicit cross-modal interactions at multiple stages. The overall workflow, shown in Fig. 2, consists of two complementary mechanisms that work together to maintain balanced modality representation. First, input features from vision and question modalities (\mathbf{F}^V and \mathbf{F}^Q) undergo Cross-Modal Prompts Query. In this stage, each modality’s features attend to the opposite modality before generating query vectors. These enriched queries are then used to select relevant prompts. Then, a mask will be applied on the weighted sum of these selected prompts to create explicit pathways for cross-modal prompts recovery. The masked prompts then first process through intra-modal recovery to establish basic modality-specific patterns while introducing light cross-modal influence, followed by cross-modal that further integrates information across modalities through attention mechanisms and selective enhancement. The result is a set of recovered prompts that maintain balanced representations from both modalities.

4 Experiment

4.1 Set Up

Dataset. Following [4], we conduct experiments on two widely-used datasets: VQA v2 [19] and NExT-QA [43]. VQA v2 contains 1.1 million pairs of real-world images and human-written questions, while NExT-QA includes 52K annotated video-based question-answer pairs. For VQA v2, we structure the continual learning experiments into 8 sequential tasks for DI and CI, while 10 sequential tasks for QI. In QI, each task introduces 1 new question type. For CI, each task contains 10 unique object classes. Under DI, each task contains 5 subtasks and each subtask focuses on 2 different question types about the same 10 object classes. For NExT-QA, we structure the experiments into 7 sequential tasks. For QI, each task introduces 1 new question type. For CI, 4 tasks contain 11 object classes each, and 3 tasks contain 12 object classes each. For DI, each task contains unique question types with 5 subtasks, where each subtask addresses the same 16 object classes.

Evaluation Metrics. We evaluate model’s performance based on two matrices: Average Performance (A), calculated as $A = \frac{1}{T} \sum_{t=1}^T \text{Acc}_{T,t}$, where $\text{Acc}_{T,t}$ means accuracy on task t after training on task T , measures overall accuracy after the training; Inter Task Forgetting (F_{inter}), computed as

Table 1: Performance comparison under DI, CI, and QI settings on VQA v2 and NExT-QA. L2P* means L2P with a single prompt pool. The best performance is highlighted in bold, and the second-best is underlined.

Method	Type	VQA v2						NExT-QA											
		DI			CI			QI			DI			CI			QI		
		$A(\uparrow)$	$F_{\text{inter}}(\downarrow)$	$F_{\text{intra}}(\downarrow)$	$A(\uparrow)$	$F_{\text{inter}}(\downarrow)$													
Dual Prompt [10]	CL	33.601	2.660	10.574	36.063	4.449	14.146	23.518	16.163	9.591	9.974	10.693	1.663	12.393	11.803				
L2P [11]	CL	31.186	2.112	12.541	33.706	4.323	13.720	23.807	14.181	9.441	9.263	9.903	1.635	10.904	10.081				
L2P* [11]	CL	31.343	2.201	12.723	33.428	4.150	13.853	23.651	14.452	9.316	9.473	10.207	1.641	11.204	10.152				
CODA [12]	CL	35.138	0.902	10.735	37.102	4.527	15.438	22.561	15.115	9.282	9.361	11.479	1.556	22.416	6.960				
Triplet [6]	CVQA	32.826	1.134	12.244	37.102	4.527	14.382	22.697	18.781	8.674	9.633	11.362	1.511	18.719	9.587				
Maple [17]	CL	35.187	1.054	11.148	37.450	4.606	15.371	22.164	17.877	8.538	9.394	11.596	1.641	16.501	10.588				
VQACL [4]	CVQA	34.224	0.867	10.626	36.950	4.431	15.525	22.452	20.472	8.772	9.041	10.787	1.818	14.870	13.500				
CluMo [9]	CVQA	35.079	1.580	11.300	36.462	4.039	13.208	25.016	18.451	9.183	8.904	11.519	1.559	17.971	11.005				
Star-prompt [13]	CL	34.437	1.784	10.584	36.516	4.172	15.104	22.837	16.695	10.347	9.218	11.030	1.742	15.571	11.750				
MM-Prompt	CVQA	36.223	0.447	10.055	39.240	3.748	16.757	21.546	22.261	8.392	8.454	13.267	1.236	24.988	6.650				

$F_{\text{inter}} = \frac{1}{T-1} \sum_{t=1}^{T-1} (\max_{j \in \{1, \dots, t\}} \text{Acc}_{j,t} - \text{Acc}_{T,t})$ quantifies the average gaps between the best performance and the current performance across tasks. In addition, for the DI setting, we introduce Inner Task Forgetting (F_{intra}), which is logically similar to the forgetting, and it specifically measures performance degradation across subtasks within a task.

Implementation Details. We construct MM-Prompt as illustrated in Fig. 2. The pretrained transformer backbone consists of 12 stacked blocks for both encoder and decoder, with each attention layer containing 12 attention heads. All experiments were conducted on a single NVIDIA RTX 4090 GPU with 24GB of memory. Following DualPrompt [10], we further divide our question and visual prompts into General (G) and Expert (E) types that target different transformer layers. We also include a weight decay [44] on the $\mathcal{L}_{\text{inter}}$ to prevent degeneration of this alignment mechanism.

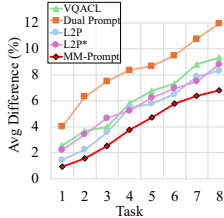
4.2 Experimental Results

In this section, we investigate and evaluate MM-Prompt against 9 outstanding and state-of-the-art methods, including 6 general CL methods [10–13, 17] and 3 CVQA methods [4, 6, 9]. For fair comparison, all models contain at least two types of prompts(Q and V) except L2P* and use approximately the same number of prompts with identical injection layers if possible.

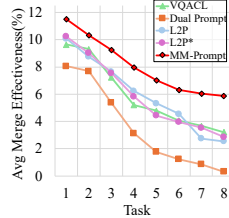
Based on Table 1, we draw several important conclusions: (1) Methods adopting cross-modal prompt isolation like Dual Prompt [10] and L2P [11] consistently show higher forgetting rates and lower accuracy across settings, confirming that isolated prompt selection and injection lead to degradation in performance due to imbalanced representations. (2) MM-Prompt consistently outperforms all the other methods across all settings. On VQA v2, it achieves 36.223% in DI (vs. MaPLe’s 35.187%), 39.240% in CI (vs. MaPLe’s 37.450%), and 16.757% in QI (vs. VQACL’s 15.525%). Notably, it reduces forgetting to less than half of the next best method in DI. On NExT-QA, MM-Prompt similarly outperforms in accuracy and maintains the lowest forgetting rates. While the second-best method varies across different incremental scenarios, MM-Prompt’s consistent superiority highlights its robustness across diverse settings. (3) We observe striking dataset-dependent difficulty patterns: VQA v2 (static images) shows poorest performance on QI, while NExT-QA (videos) struggles most with CI, suggesting that temporal dynamics fundamentally alter how modality conflicts during continual learning. (4) Among comparison methods, MaPLe [17] performs relatively well, which we attribute to its gradient-based visual-linguistic interactions. (5) Specialized CVQA methods like Triplet [6] and VQACL [4] underperform despite their success in classification-based settings and with memory buffers, highlighting MM-Prompt’s efficiency for maintaining balanced representations across modalities. These results collectively validate our approach’s effectiveness in maintaining balanced cross-modal representations across diverse incremental learning scenarios.

4.3 Modality Integration Analysis

To demonstrate that isolated prompts amplify modality imbalance, we train the models as normal and evaluate them on joint, vision-only and question-only inputs, then compute Modality Merge Effectiveness and Modality Difference, details for these settings are in Appendix A. As shown in Fig. 3, existing prompt-based methods [4, 10, 11] that adopt cross modal prompts isolation show low merge effectiveness and high modality gaps during the continual learning process. In contrast, our method

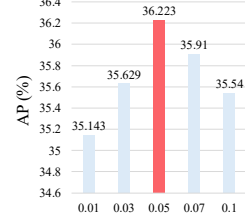


(a) Modality Difference

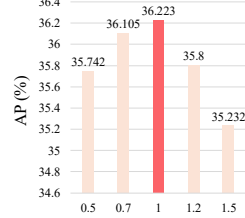


(b) Modality Merge

Figure 3: Comparison between existing prompt-based approaches and our MM-Prompt model.



(a) Effect of different δ



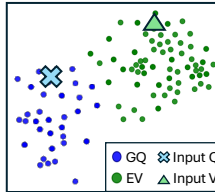
(b) Effect of different α

Figure 4: Performance variation under different masking and cross alignment loss ratio on VQA v2.

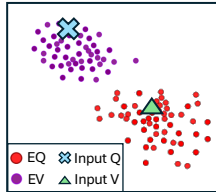
maintains consistently high merge effectiveness and minimal modality disparity across new tasks, while achieving superior overall accuracy. These improvements stem from our two-component design: cross-modal prompt query prevents selection bias by enriching queries with complementary information, while cross-modal prompt recovery creates explicit pathways for modality interaction and fulfill them with cross-modal information. Together, these mechanisms counteract modality imbalance at critical points where isolation typically occurs in existing methods.



Figure 5: Bottom up attention visualization[45] during inference on Dual Prompt [10] and MM-Prompt.



(a) Dual Prompt[10] ($A : 33.601, F_{\text{inter}} : 2.660$)



(b) MM-Prompt ($A : 36.223, F_{\text{inter}} : 0.447$)

Figure 6: Visualization of injected prompts and input feature using t-SNE [46].

Figs. 5 and 6 provide further qualitative evidence. We visualize the attention from the model on the bounding boxes during the inference using [45]. The attention maps (Fig. 5) show MM-Prompt precisely focuses on relevant image regions (correctly identifying “broccoli” and “airport”), while existing methods such as Dual Prompt produce incorrect answers with diffuse attention patterns, indicating possible occurrence of modality bias [18]. The t-SNE visualization [46] of injected prompts (Fig. 6) confirms the cross-modal merging effectiveness of MM-Prompt. As shown in Fig. 6b, MM-Prompt’s prompts form more tightly assembled clusters compared to Dual Prompt in Fig. 6a, where prompts remain clearly separated by modality. This observation demonstrates how our cross-modal prompt query and recover mechanisms help prompts encode integrated information across modalities rather than remaining isolated within modality-specific subspaces. Additionally, examining the input features from the question “What green vegetable is on the plate?” in Fig. 5 reveals another key difference: in MM-Prompt, input features position at the intersection between Q and V prompt clusters, while prompts in Dual Prompt remain distinctly separated by modality. This demonstrates that MM-Prompt’s injected prompts contains shared representational properties that facilitate effective cross-modal understanding and prevent modality-isolated prompts throughout sequential learning.

4.4 Ablation Study

Impact of Hyperparameters. We evaluate MM-Prompt’s sensitivity to two key hyperparameters in Fig. 4. For mask ratio (δ), which controls the proportion of prompt tokens masked for recovery, we observed that too few masking ($\delta = 0.01$) is insufficient for prompts to effectively incorporate cross-

Table 2: Performance comparison of different methods on NExT-QA dataset under DI setting with memory usage (Mem).

Methods	NExT-QA		
	Mem	$A (\uparrow)$	$F_{\text{inter}} (\downarrow)$
Triplet [6]	500	27.996	3.282
Dual Prompt [10]	500	27.641	3.765
CODA [12]	500	30.632	2.471
Maple[17]	500	30.049	3.112
VQACL [4]	500	30.753	2.692
CluMo [9]	500	29.776	3.248
MM-Prompt	500	32.394	2.259
MM-Prompt	200	29.945	3.112
MM-Prompt	1000	34.268	2.427

modal information, resulting in weaker performance. Conversely, excessive masking ($\delta = 0.10$) creates too many information gaps, making results unstable and hard to reproduce. The optimal value ($\delta = 0.05$) balances these constraints, creating sufficient recovery opportunities while maintaining enough context for effective learning. Similarly, for the inter alignment loss weight (α), we find moderate values perform best, with peak performance at $\alpha = 1.0$. Lower values provide insufficient cross-modal alignment constraints, failing to effectively counter modality isolation. Higher values ($\alpha > 1.2$) divert the model’s focus from generate correct answers to alignment, degrading task performance by over-emphasizing representational similarity.

Impact of Task Order. Figs. 8a and 8b demonstrate MM-Prompt’s stability across different learning scenarios. MM-Prompt maintains more consistent performance across different task orders, while Dual Prompt[10] exhibits more varied performance. By maintaining balanced representations through explicit cross-modal pathways in injected prompts, MM-Prompt reduces the cascading effects of task order biases that typically compound in existing prompt methods. This order-invariant behavior strongly evidences that MM-Prompt successfully maintains balanced representations throughout the continual learning process.

Effect of Components To evaluate MM-Prompt’s design, we conducted an ablation study with sequential component addition (Table 3). The baseline achieves 34.172% accuracy with 1.31 forgetting. Adding cross-modal prompt query (Eqs. (1) and (3)) improves accuracy to 34.990% and significantly reduces forgetting to 0.588, confirming the importance of cross-modal awareness during selection. The complete MM-Prompt with cross-modal prompt recovery (Eqs. (4) to (10)) achieves the best performance with 36.223% accuracy and 0.447 forgetting, demonstrating the effectiveness for creating explicit pathways to let prompts learn complementary information from the other modality. Together, these results reveal the complementary nature of our two components and confirm the importance of cross-modal aware prompts.

Performance with Memory Buffer For NExT-QA dataset, which contains complex video question-answering tasks with longer sequences and fewer training data, we also evaluate models with a memory buffer of 500 samples (Table 2). As a result, MM-Prompt substantially outperforms all the other methods, given that all methods benefit from the same memory capacity. These results confirm that MM-Prompt’s approach to create explicit pathways for modality interaction remain effective when supplemented with traditional continual learning techniques [26, 27].

Computational Efficiency. Fig. 7 shows that the inference efficiency of MM-Prompt remains competitive with existing methods. Processing 100 samples takes 0.179 seconds, which is more efficient than MAPLE [17] (0.211s) and TRIPLET [6] (0.226s), while only slightly slower than Dual Prompt [10] (0.158s). This modest computational overhead delivers substantial performance improvements and significant forgetting reduction compared to the Dual Prompt [10]. This demonstrates that fostering the cross-modal understanding can be achieved with reasonable computational costs, making MM-Prompt practical for real-world continual learning applications.

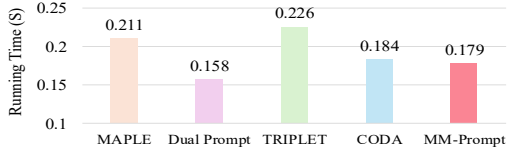
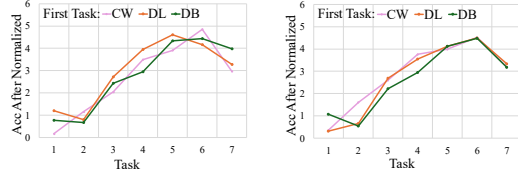


Figure 7: Time spent processing 100 samples.



(a) Dual Prompt [10] (b) MM-Prompt

Figure 8: Comparison with different task orders in NExT QA under DI setting.

Table 3: Ablation study on VQA v2 under DI setting showing the effects of CQ: cross-modal prompt query, CR: cross-modal prompt recovery

CQ	CR	$A (\uparrow)$	$F_{\text{inter}} (\downarrow)$
		34.172	1.310
✓		34.990	0.588
✓	✓	36.223	0.447

5 Conclusion

Conclusion. This paper presents MM-Prompt, a novel prompt-based framework for CVQA that explicitly addresses the overlooked issue of cross-modal prompt isolation. While existing methods rely on independently selected visual and textual prompts, they often worsen modality imbalance. MM-Prompt introduces a unified solution that promotes balanced and integrated cross-modal reasoning. Through two key components, cross-modal prompt query, which injects complementary modality cues into prompt selection, and cross-modal prompt recovery, which reconstructs shared representations via structured masking and hierarchical integration, MM-Prompt enables consistent fusion of multi-modal knowledge. Extensive experiments on VQA v2 and NExT-QA under various continual learning settings demonstrate that MM-Prompt achieves superior performance, enhanced modality balance, and reduced forgetting. These results confirm that addressing prompt isolation is critical for long-term, robust multi-modal learning.

Limitations. The current masking strategy is random, which, in a multi-modal setting, may result in the loss of important information and hinder effective training. Future work could explore adaptive and context-aware masking strategies that dynamically preserve critical cross-modal content based on different task scenarios.

References

- [1] Yuanze Lin, Yujia Xie, Dongdong Chen, Yichong Xu, Chenguang Zhu, and Lu Yuan. RE-VIVE: Regional visual representation matters in knowledge-based visual question answering. In *Advances in Neural Information Processing Systems (NeurIPS)*, pages 10560–10571, 2022.
- [2] Sahithya Ravi, Aditya Chinchure, Leonid Sigal, Renjie Liao, and Vered Shwartz. VLC-BERT: Visual question answering with contextualized commonsense knowledge. In *Proceedings of the IEEE/CVF Winter Conference on Applications of Computer Vision (WACV)*, pages 1155–1165, 2023.
- [3] Junnan Li, Ramprasaath Selvaraju, Akhilesh Gotmare, Shafiq Joty, Caiming Xiong, and Steven Chu Hong Hoi. Align before fuse: Vision and language representation learning with momentum distillation. In *Advances in Neural Information Processing Systems (NeurIPS)*, pages 9694–9705, 2021.
- [4] Xi Zhang, Feifei Zhang, and Changsheng Xu. Vqacl: A novel visual question answering continual learning setting. In *Proceedings of the IEEE/CVF Conference on Computer Vision and Pattern Recognition (CVPR)*, pages 19102–19112, 2023.
- [5] Malvina Nikandrou, Georgios Pantazopoulos, Ioannis Konstas, and Alessandro Soglia. Enhancing continual learning in visual question answering with modality-aware feature distillation. *arXiv preprint arXiv:2406.19297*, 2024.
- [6] Zi Qian, Xin Wang, Xuguang Duan, Pengda Qin, Yuhong Li, and Wenwu Zhu. Decouple before interact: Multi-modal prompt learning for continual visual question answering. In *Proceedings of the IEEE/CVF International Conference on Computer Vision (ICCV)*, pages 2953–2962, 2023.
- [7] Yuanze Lin, Yujia Xie, Dongdong Chen, Yichong Xu, Chenguang Zhu, and Lu Yuan. RE-VIVE: Regional visual representation matters in knowledge-based visual question answering. In *Advances in Neural Information Processing Systems (NeurIPS)*, pages 10560–10571, 2022.
- [8] Stan Weixian Lei, Difei Gao, Jay Zhangjie Wu, Yuxuan Wang, Wei Liu, Mengmi Zhang, and Mike Zheng Shou. Symbolic replay: Scene graph as prompt for continual learning on VQA task. In *Proceedings of the AAAI Conference on Artificial Intelligence (AAAI)*, pages 139–149, 2023.
- [9] Yuliang Cai and Mohammad Rostami. CluMo: Cluster-based modality fusion prompt for continual learning in visual question answering. *arXiv preprint arXiv:2408.11742*, 2024.
- [10] Zifeng Wang, Zizhao Zhang, Sayna Ebrahimi, Ruoxi Sun, Han Zhang, Chen-Yu Lee, Xiaoqi Ren, Guolong Su, Vincent Perot, Jennifer Dy, et al. DualPrompt: Complementary prompting for rehearsal-free continual learning. In *European Conference on Computer Vision (ECCV)*, pages 631–648. Springer, 2022.
- [11] Zifeng Wang, Zizhao Zhang, Chen-Yu Lee, Han Zhang, Ruoxi Sun, Xiaoqi Ren, Guolong Su, Vincent Perot, Jennifer Dy, and Tomas Pfister. Learning to prompt for continual learning. In *Proceedings of the IEEE/CVF Conference on Computer Vision and Pattern Recognition (CVPR)*, pages 139–149, 2022.
- [12] James Seale Smith, Leonid Karlinsky, Vyshnavi Gutta, Paola Cascante-Bonilla, Donghyun Kim, Assaf Arbelle, Rameswar Panda, Rogerio Feris, and Zsolt Kira. CODA-Prompt: Continual decomposed attention-based prompting for rehearsal-free continual learning. In *Proceedings of the IEEE/CVF Conference on Computer Vision and Pattern Recognition (CVPR)*, pages 11909–11919, 2023.
- [13] Martin Menabue, Emanuele Frascaroli, Matteo Boschini, Enver Sangineto, Lorenzo Bonicelli, Angelo Porrello, and Simone Calderara. Semantic residual prompts for continual learning. In *European Conference on Computer Vision (ECCV)*, pages 1–18. Springer, 2024.
- [14] Fan Lyu, Shuai Wang, Wei Feng, Zihan Ye, Fuyuan Hu, and Song Wang. Multi-domain multi-task rehearsal for lifelong learning. In *Proceedings of the AAAI Conference on Artificial Intelligence (AAAI)*, pages 8819–8827, 2021.

[15] Qing Sun, Fan Lyu, Fanhua Shang, Wei Feng, and Liang Wan. Exploring example influence in continual learning. 2022.

[16] Fan Lyu, Qing Sun, Fanhua Shang, Liang Wan, and Wei Feng. Measuring asymmetric gradient discrepancy in parallel continual learning. In *Proceedings of the IEEE/CVF International Conference on Computer Vision (ICCV)*, pages 11411–11420, 2023.

[17] Muhammad Uzair Khattak, Hanoona Rasheed, Muhammad Maaz, Salman Khan, and Fa-had Shahbaz Khan. MAPLE: Multi-modal prompt learning. In *Proceedings of the IEEE/CVF Conference on Computer Vision and Pattern Recognition (CVPR)*, pages 19113–19122, 2023.

[18] Sainandan Ramakrishnan, Aishwarya Agrawal, and Stefan Lee. Overcoming language priors in visual question answering with adversarial regularization. In *Advances in Neural Information Processing Systems (NeurIPS)*, page 152–164, 2018.

[19] Yash Goyal, Tejas Khot, Douglas Summers-Stay, Dhruv Batra, and Devi Parikh. Making the v in VQA matter: Elevating the role of image understanding in visual question answering. In *Proceedings of the IEEE Conference on Computer Vision and Pattern Recognition (CVPR)*, pages 6904–6913, 2017.

[20] Stanislaw Antol, Aishwarya Agrawal, Jiasen Lu, Margaret Mitchell, Dhruv Batra, C. Lawrence Zitnick, and Devi Parikh. VQA: Visual question answering. In *Proceedings of the IEEE International Conference on Computer Vision (ICCV)*, pages 2425–2433, 2015.

[21] Sebastian Thrun. A lifelong learning perspective for mobile robot control. In *Proceedings of the IEEE/RSJ International Conference on Intelligent Robots and Systems (IROS)*, pages 201–214, 1995.

[22] Zangwei Zheng, Mingyuan Ma, Kai Wang, Ziheng Qin, Xiangyu Yue, and Yang You. Preventing zero-shot transfer degradation in continual learning of vision-language models. In *Proceedings of the IEEE/CVF International Conference on Computer Vision (ICCV)*, pages 19125–19136, 2023.

[23] Mingrui Lao, Nan Pu, Yu Liu, Zhun Zhong, Erwin M. Bakker, Nicu Sebe, and Michael S. Lew. Multi-domain lifelong visual question answering via self-critical distillation. In *Proceedings of the 31st ACM International Conference on Multimedia (ACM MM)*, pages 4747–4758, 2023.

[24] Jiazu Yu, Yunzhi Zhuge, Lu Zhang, Ping Hu, Dong Wang, Huchuan Lu, and You He. Boosting continual learning of vision-language models via mixture-of-experts adapters. In *Proceedings of the IEEE/CVF Conference on Computer Vision and Pattern Recognition (CVPR)*, pages 23219–23230, 2024.

[25] Xilai Li, Yingbo Zhou, Tianfu Wu, Richard Socher, and Caiming Xiong. Learn to grow: A continual structure learning framework for overcoming catastrophic forgetting. In *Proceedings of the International Conference on Machine Learning (ICML)*, pages 3925–3934. PMLR, 2019.

[26] David Rolnick, Arun Ahuja, Jonathan Schwarz, Timothy Lillicrap, and Gregory Wayne. Experience replay for continual learning. In *Advances in Neural Information Processing Systems (NeurIPS)*, pages 348–358, 2019.

[27] Pietro Buzzega, Matteo Boschini, Angelo Porrello, Davide Abati, and Simone Calderara. Dark experience for general continual learning: A strong, simple baseline. In *Advances in Neural Information Processing Systems (NeurIPS)*, pages 15920–15930, 2020.

[28] Matthias De Lange, Rahaf Aljundi, Marc Masana, Sarah Parisot, Xu Jia, Aleš Leonardis, Gregory Slabaugh, and Tinne Tuytelaars. A continual learning survey: Defying forgetting in classification tasks. *IEEE Transactions on Pattern Analysis and Machine Intelligence*, pages 3366–3385, 2021.

[29] Dianzhi Yu, Xinni Zhang, Yankai Chen, Aiwei Liu, Yifei Zhang, Philip S. Yu, and Irwin King. Recent advances of multimodal continual learning: A comprehensive survey. *arXiv preprint arXiv:2410.05352*, 2024.

[30] Xiaokang Peng, Yake Wei, Andong Deng, Dong Wang, and Di Hu. Balanced multimodal learning via on-the-fly gradient modulation. In *Proceedings of the IEEE/CVF Conference on Computer Vision and Pattern Recognition (CVPR)*, pages 8238–8247, 2022.

[31] Xu Han, Zhengyan Zhang, Ning Ding, Yuxian Gu, Xiao Liu, Yuqi Huo, Jiezhong Qiu, Yuan Yao, Ao Zhang, Liang Zhang, et al. Pre-trained models: Past, present and future. *AI Open*, pages 225–250, 2021.

[32] Colin Raffel, Noam Shazeer, Adam Roberts, Katherine Lee, Sharan Narang, Michael Matena, Yanqi Zhou, Wei Li, and Peter J. Liu. Exploring the limits of transfer learning with a unified text-to-text transformer. *Journal of Machine Learning Research*, pages 1–67, 2020.

[33] Hao Tan and Mohit Bansal. LXMERT: Learning cross-modality encoder representations from transformers. *arXiv preprint arXiv:1908.07490*, 2019.

[34] Arthur Douillard, Alexandre Ramé, Guillaume Couairon, and Matthieu Cord. DyTox: Transformers for continual learning with dynamic token expansion. In *Proceedings of the IEEE/CVF Conference on Computer Vision and Pattern Recognition (CVPR)*, pages 9285–9295, 2022.

[35] Alec Radford, Jong Wook Kim, Chris Hallacy, Aditya Ramesh, Gabriel Goh, Sandhini Agarwal, Girish Sastry, Amanda Askell, Pamela Mishkin, Jack Clark, et al. Learning transferable visual models from natural language supervision. In *Proceedings of the International Conference on Machine Learning (ICML)*, pages 8748–8763. PMLR, 2021.

[36] Yubo Chang, Fan Lyu, Zhang Zhang, and Liang Wang. Understanding driving risks via prompt learning. In *IEEE International Conference on Systems, Man, and Cybernetics (SMC)*, pages 3637–3642, 2024.

[37] Arsha Nagrani, Shan Yang, Anurag Arnab, Aren Jansen, Cordelia Schmid, and Chen Sun. Attention bottlenecks for multimodal fusion. In *Advances in Neural Information Processing Systems (NeurIPS)*, 2021.

[38] Mingrui Wu, Xuying Zhang, Xiaoshuai Sun, Yiyi Zhou, Chao Chen, Jiaxin Gu, Xing Sun, and Rongrong Ji. Difnet: Boosting visual information flow for image captioning. In *Proceedings of the IEEE/CVF conference on computer vision and pattern recognition (CVPR)*, 2022.

[39] Fenglin Liu, Yuanxin Liu, Xuancheng Ren, Xiaodong He, and Xu Sun. Aligning visual regions and textual concepts for semantic-grounded image representations. In *Advances in Neural Information Processing Systems (NeurIPS)*, 2019.

[40] Kaiming He, Xinlei Chen, Saining Xie, Yanghao Li, Piotr Dollár, and Ross Girshick. Masked autoencoders are scalable vision learners. In *Proceedings of the IEEE/CVF Conference on Computer Vision and Pattern Recognition (CVPR)*, pages 16000–16009, 2022.

[41] Chaoning Zhang, Chenshuang Zhang, Junha Song, John Seon Keun Yi, Kang Zhang, and In So Kweon. A survey on masked autoencoder for self-supervised learning in vision and beyond. *arXiv preprint arXiv:2208.00173*, 2022.

[42] Nitin Bansal, Xiaohan Chen, and Zhangyang Wang. Can we gain more from orthogonality regularizations in training deep networks? In *Advances in Neural Information Processing Systems (NeurIPS)*, 2018.

[43] Junbin Xiao, Xindi Shang, Angela Yao, and Tat-Seng Chua. NExT-QA: Next phase of question answering to explaining temporal actions. In *Proceedings of the IEEE/CVF Conference on Computer Vision and Pattern Recognition (CVPR)*, pages 9777–9786, 2021.

[44] Anders Krogh and John Hertz. A simple weight decay can improve generalization. In *Advances in Neural Information Processing Systems (NeurIPS)*, pages 950–957, 1991.

[45] Peter Anderson, Xiaodong He, Chris Buehler, Damien Teney, Mark Johnson, Stephen Gould, and Lei Zhang. Bottom-up and top-down attention for image captioning and visual question answering. In *Proceedings of the IEEE Conference on Computer Vision and Pattern Recognition (CVPR)*, pages 6077–6086, 2018.

- [46] Laurens Van der Maaten and Geoffrey Hinton. Visualizing data using t-SNE. *Journal of Machine Learning Research*, pages 2579–2605, 2008.
- [47] Hyung Won Chung, Le Hou, Shayne Longpre, Barret Zoph, Yi Tay, William Fedus, Yunxuan Li, Xuezhi Wang, Mostafa Dehghani, Siddhartha Brahma, et al. Scaling instruction-finetuned language models. *Journal of Machine Learning Research*, 2024.
- [48] Mike Lewis, Yinhan Liu, Naman Goyal, Marjan Ghazvininejad, Abdelrahman Mohamed, Omer Levy, Veselin Stoyanov, and Luke Zettlemoyer. BART: Denoising sequence-to-sequence pre-training for natural language generation, translation, and comprehension. In *Proceedings of the Annual Meeting of the Association for Computational Linguistics (ACL)*, pages 7871–7880, 2020.

A Datasets used in Our Work

A.1 Dataset Partitioning

For VQA v2 [19], we organize the continual learning experiments into 8 sequential tasks for both Class Increment (CI) and Dual Increment (DI) settings. In the CI setting, each task introduces 10 unique object classes. In the DI setting, each task consists of 5 subtasks, each focusing on 2 distinct question types about the same 10 object classes. For the Question Increment (QI) setting, we define 10 sequential tasks, each introducing 1 new question type.

For NExT-QA [43], we structure the experiments into 7 sequential tasks due to the dataset’s scale. In the QI setting, each task introduces 1 new question type. In the CI setting, 4 tasks contain 11 object classes each, while the remaining 3 tasks contain 12 object classes each. In the DI setting, each task consists of 5 subtasks with unique question types, each subtask cover 16 different object classes.

Table 4: Object class increment in VQA v2 for CI and DI.

Task	Objects
Group 1	truck, couch, bowl, chair, scissors, sandwich, orange, knife, dining table, potted plant
Group 2	teddy bear, microwave, skateboard, bottle, hot dog, book, apple, refrigerator, tennis racket, oven
Group 3	laptop, person, car, banana, snowboard, bed, umbrella, surfboard, motorcycle, sink
Group 4	tv, dog, baseball bat, cup, parking meter, sheep, spoon, cake, broccoli, toilet
Group 5	kite, fork, bus, train, cell phone, pizza, keyboard, sports ball, cow, giraffe
Group 6	baseball glove, bear, wine glass, traffic light, horse, mouse, stop sign, zebra, handbag, skis
Group 7	fire hydrant, toaster, cat, bench, remote, clock, hair drier, bird, suitcase, toothbrush
Group 8	carrot, backpack, tie, elephant, frisbee, bicycle, donut, boat, airplane, vase

A.2 Partitioning Details and Group Definitions

For VQA v2, we structure the continual learning experiments into 8 sequential tasks for DI and CI, while QI has 10 sequential tasks due to the total number of question types. Tables 4, 6, and 7 provide details on the distribution of object classes and question types across these tasks. In the DI setting, tasks follow the class distribution outlined in Table 4, with each task further divided into 5 subtasks according to the question type distribution in Table 6. For the CI setting, we directly implement the class grouping specified in Table 4 while maintaining all question types across each task. In the QI setting, we utilize the question grouping from Table 7, while keeping object classes consistent across all tasks.

For NExT-QA [43], we structure the experiments into 7 sequential tasks following the approach of [4]. In the DI setting, we implement the hierarchical structure defined in [4], with question increments ordered according to Table 8. For the QI setting, we utilize the question type ordering specified in Table 8 while maintaining consistent visual classes across all tasks. In the CI setting, we employ the object class groups outlined in Table 5 while preserving all question types throughout the tasks.

Table 5: Object classes increment in NExT-QA for CI.

Task	Objects
Group 1	bicycle, camel, bat, microwave, snake, sofa, traffic light, hamster/rat, chicken, oven, stop sign
Group 2	crab, camera, lion, ball/sports ball, crocodile, screen/monitor, baby walker, cat, squirrel, frisbee, cattle/cow
Group 3	piano, watercraft, kangaroo, train, fruits, pig, suitcase, bear, tiger, bench, elephant
Group 4	ski, stingray, antelope, toy, child, duck, guitar, dish, fish, cake, turtle, leopard
Group 5	penguin, faucet, car, bottle, bus/truck, aircraft, baby, bread, baby seat, cell-phone, sink, rabbit
Group 6	vegetables, skateboard, bird, toilet, racket, sheep/goat, adult, scooter, electric fan, stool, motorcycle
Group 7	horse, snowboard, surfboard, handbag, laptop, panda, table, cup, backpack, chair, dog, refrigerator

B Detailed Component Analysis

B.1 Modality Merge Effectiveness and Modality Difference

In Section 4.3, we use Modality Merge Effectiveness and Modality Difference to demonstrate that isolated prompts amplify modality imbalance. To get these two matrices, we train models under the standard setting and evaluate them using three input configurations, joint, vision-only, and question-only. Remind that \mathbf{F}^Q and \mathbf{F}^V denote the question and vision features, $\mathbf{p}_{\text{final}}^Q$ and $\mathbf{p}_{\text{final}}^V$ represents the final question and vision prompts that will be injected to the encoder.

In the joint setting, both modality features \mathbf{F}^Q and \mathbf{F}^V , as well as the final prompts $\mathbf{p}_{\text{final}}^Q$ and $\mathbf{p}_{\text{final}}^V$, are available to the model. The vision-only setting provides only \mathbf{F}^V and $\mathbf{p}_{\text{final}}^V$, while the question-only setting provides only \mathbf{F}^Q and $\mathbf{p}_{\text{final}}^Q$. To quantify modality interaction and imbalance, we compute:

$$\text{Modality Merge Effectiveness} = \text{Acc}^{\text{Joint}} - \max(\text{Acc}^{\text{V-Only}}, \text{Acc}^{\text{Q-Only}}). \quad (12)$$

This metric quantifies the additional information gained through cross-modal integration. Higher values indicate the model effectively leverages complementary signals from both modalities beyond what either modality provides alone.

$$\text{Modality Difference} = \max(\text{Acc}^{\text{V-Only}}, \text{Acc}^{\text{Q-Only}}) - \min(\text{Acc}^{\text{V-Only}}, \text{Acc}^{\text{Q-Only}}). \quad (13)$$

This metric measures the performance gap between modalities, where higher values indicate greater reliance on the dominant modality, while lower values reflect more balanced representations across the two modalities.

Ideally, a model should maximize Merge Effectiveness while minimizing Modality Difference. MM-Prompt achieves consistently higher Modality Merge Effectiveness and lower Modality Difference across sequential tasks compared to all baseline methods. This quantitative evidence confirms that our approach not only maintains more balanced representations of both modalities but also more effectively integrates complementary information across them. These results further validate our design choices: Cross-Modal Prompt Query ensures prompts inherently carry the cross-modal information, while Cross-Modal Prompt Recovery reinforces integration through explicit information exchange pathways, together creating a robust defense against the modality imbalance that typically accumulates in continual learning scenarios.

B.2 Insertion Layers and Number of Prompts

Following [10], we insert General prompts at lower layers {1,2} and Expert prompts at intermediate layers {3,4,5}. This configuration follows the hierarchical processing pattern of the transformer, where lower layers handle more specific, fine-grained patterns, while intermediate layers process more abstract, transferable representations.

Table 6: Question types increment in VQA v2 for DI.

Task	Group 1	Group 2	Group 3	Group 4	Group 5
Question Types	Recognition Location	Judge Commonsense	Count Action	Color Type	Subcategory Causal

Table 7: Question types increment in VQA v2 for QI.

Task	Group 1	Group 2	Group 3	Group 4	Group 5
Question Type	Recognition	Location	Judge	Commonsense	Count
Task	Group 6	Group 7	Group 8	Group 9	G10
Question Type	Action	Color	Type	Subcategory	Causal

Table 8: Question types increment in NExT-QA for QI and DI.

Task	Group 1	Group 2	Group 3	Group 4	Group 5	Group 6	Group 7
Question Type	CW	TN	TC	DL	DB	DC	DO

As shown in Table 9, we set the number of prompts to be QG=40, QV=60, EG=80, EV=120, allocating more capacity to visual prompts and expert prompts, as there are more object classes than question types in the dataset. The larger number of Expert prompts enables more specialized handling of diverse visual concepts and complex reasoning patterns, improving the model’s ability to adapt to new tasks. Notably, simply increasing prompt counts (60,80,100,140) decreases performance, suggesting that excessive prompt quantities can lead to lower representation quality and slower convergence.

B.3 Intra and Inter Modal Recovery Analysis

Table 10 presents an ablation study examining the contribution of each recovery step to MM-Prompt’s performance. The baseline model with only cross-modal query achieves 34.990% AP with 0.588 forgetting. Adding only intra-modal recovery marginally improves accuracy to 35.150% but substantially worsens forgetting to 1.140, nearly doubling the forgetting rate. This reveals a key insight that intra-modal recovery alone may intensify the modality imbalance problem by strengthening modality-specific patterns without proper cross-modal integration. On the other hand, without the intra-modal phase to first preserve and emphasize essential modality-specific characteristics, inter-modal recovery causes premature mixing where important uni-modal patterns are lost or dominated by the stronger modality before they can be properly established. When both phases are applied, we can see significant improvements in both metrics (36.223% AP, 0.447 forgetting). This demonstrates that balanced cross-modal representations require both the preservation of modality-specific characteristics provided by intra-modal recovery and explicit pathways for cross-modal integration provided by inter-modal recovery, working together to overcome the isolation problem that undermines existing approaches.

Table 11 demonstrates the importance of both $\mathcal{L}_{\text{intra}}$ and $\mathcal{L}_{\text{inter}}$ for effective prompt recovery. Without any alignment losses, the model achieves only 34.260% accuracy with high forgetting (1.871), as the recovery process lacks proper guidance and may not be able to reconstruct any meaningful information. The $\mathcal{L}_{\text{intra}}$ ensures accurate reconstruction of modality-specific patterns, preserving essential characteristics of each modality. Without this foundation, the model would struggle to maintain the fundamental representation structure needed for effective reasoning within each modality. Meanwhile, the $\mathcal{L}_{\text{inter}}$ explicitly guides cross-modal interaction, preventing one modality from dominating the recovery process and ensuring balanced integration. Only when both losses work together, the model achieves the optimal performance by simultaneously preserving modality-specific characteristics while enforcing balanced cross-modal integration.

Fig. 9 shows the effect of different $\mathcal{L}_{\text{intra}}$ ratios. Similar to the ratio for $\mathcal{L}_{\text{inter}}$, the moderate value still performs the best, with peak performance at $\alpha = 0.3$. Lower values provide insufficient reconstruction guidance, fail to reconstruct the original representations. Higher values shift the model’s

Table 9: Effect of different number of prompts in the order of QG, QE, VG, VE.

Number of Prompts	$A (\uparrow)$	$F_{\text{inter}}(\downarrow)$
10,80,10,80	35.79	0.914
50,50,50,50	35.168	1.268
40,60,80,120	36.223	0.447
60,80,100,140	34.851	0.985

Table 10: Performance variation for different recovery phases.

Intra	Inter	$A (\uparrow)$	$F_{\text{inter}}(\downarrow)$
		34.990	0.588
✓		35.150	1.140
	✓	35.318	1.071
✓	✓	36.223	0.447

focus away from producing correct answers to enforcing alignment, which harms task performance by placing excessive emphasis on representational similarity.

B.4 Comparisons with Other Fusion Strategies

Tables 12 and 13 present comprehensive analysis of different modality interaction strategies at the query stage and before the injection stage. In Table 12, we compare our cross-modal prompt query against simpler integration methods. Naive strategies like “Plus”, “Mean Pooling” and “Hadamard Product” directly combining features from both modalities achieve low accuracy with high forgetting, as a simple combination provides no mechanism to balance the influence of the dominant modality, which can overwhelm the joint representation. The standard “Cross Attention” approach improves performance moderately by allowing selective feature integration, but still permits the dominant modality’s features to disproportionately influence attention weights and outputs. In contrast, our cross-modal prompt query approach with controlled residual connections and learnable modulation weights outperforms all the alternatives by maintaining essential modality-specific characteristics while enabling balanced cross-modal influence.

Table 13 further demonstrates that our structured approach for prompt recovery is equally crucial. Cross-modal prompt recovery creates explicit pathways for cross-modal information integration. Our recovery method first establishes modality-specific foundations before progressively integrating cross-modal information through controlled pathways. This structured approach preserves essential characteristics of each modality while enabling targeted information exchange. Unlike the naive combination methods that allow dominant signals to overwhelm the integration process, our method creates explicit, balanced pathways for cross-modal information flow.

Notably, the “Plus” operation yields the lowest performance in both stages, suggesting that simply adding the prompts together can significantly diminishes the complementary information provided by the vision modality. These results confirm that both components of cross-modal prompt query and cross modal prompt recovery complementarily creating prompts with effective cross-modal awareness, thus achieve the best performance.

C More Visualization

C.1 Heatmap Comparison

As illustrated in Fig. 10, MM-Prompt consistently directs attention to relevant regions, while Dual Prompt often diffuses or drifts focus, leading to incorrect predictions. In Example 1, MM-Prompt focus on the aircraft in the sky and generate the correct answer “plane” while Dual Prompt attends to an edge of the wing and misclassifies it as “bird”. A similar pattern holds in Example 2, MM-Prompt highlights both animals and counts “2” whereas Dual Prompt spreads attention across the pasture and under-counts. In Example 3, where fine-grained localization is required, MM-Prompt put the attention on the frisbee in the man’s hand and answers correctly, contrasting with Dual Prompt’s off-

Table 11: Performance variation for different alignment loss

$\mathcal{L}_{\text{intra}}$	$\mathcal{L}_{\text{inter}}$	$A (\uparrow)$	$F_{\text{inter}}(\downarrow)$
		34.260	1.871
✓		34.743	1.531
	✓	35.059	1.204
✓	✓	36.223	0.447

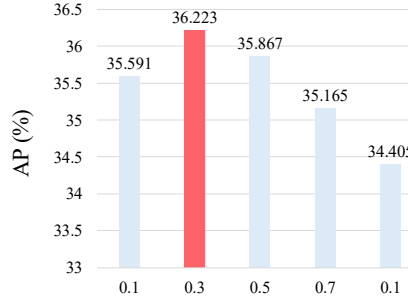


Figure 9: Effect of different $\mathcal{L}_{\text{intra}}$ ratio.

target focus that yields “no”. These patterns persist across other tasks involving abstract reasoning and lighting assessment. These improvements arise from the design of MM-Prompt, where cross-modal prompt query enriches queries with complementary cues and cross-modal prompt recovery established explicit pathways for modality interaction. Together, these mechanisms create prompts with cross-modal awareness, thus counteract modality imbalance and improve performance.

C.2 Failure Case

Despite MM-Prompt’s overall strong performance, we acknowledge several failure cases that highlight remaining challenges in cross-modal reasoning shown in Fig. 11. In Example 1, when asked “What is in the blue pot?”, MM-Prompt incorrectly focus on the black pot instead of the deep blue one, showing difficulty distinguishing between objects with similar colors. Example 2 reveals limitations with shape reasoning, where the model incorrectly identifies a round cake as “square”, which is likely due to our bounding box feature representation that cannot properly capture circular shapes. Example 3 demonstrates challenges with spatial reasoning in the question “Are the people nearest the camera riding bicycles?”, where attention focuses on the wrong individuals, suggesting difficulty with multi-step reasoning.

These failure cases point to specific areas for future improvement. (1) more adaptive masking strategies that align better with the case-specific settings, (2) more advanced visual feature representations beyond bounding boxes to better capture shape information. These enhancements would strengthen MM-Prompt’s ability to maintain balanced cross-modal representations while addressing specific reasoning challenges.

Table 12: Comparisons of different multi-modal fusion strategies during the query stage.

Strategy	$A (\uparrow)$	$F_{\text{inter}} (\downarrow)$
Plus	34.275	1.731
Mean Pooling	34.398	2.015
Hadamard Product	34.702	1.142
Cross Attention	34.891	1.202
Ours' Query	36.223	0.447

Table 13: Performance variation under different strategies of modality interaction before prompt injection.

Strategy	$A (\uparrow)$	$F_{\text{inter}} (\downarrow)$
Plus	33.850	1.335
Mean Pooling	34.170	1.405
Hadamard Product	34.212	1.274
Cross Attention	34.628	1.428
Our Recovery	36.223	0.447

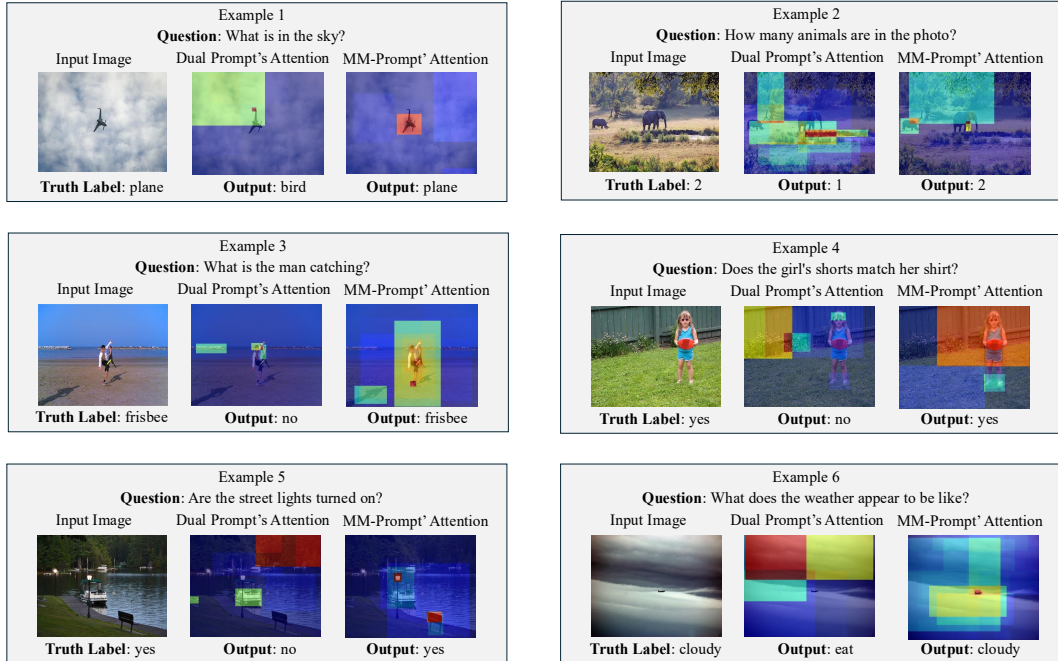


Figure 10: Bottom up attention visualization[45] during inference on Dual Prompt [10] and MM-Prompt.

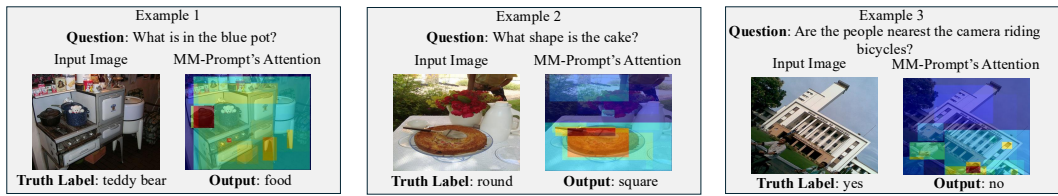


Figure 11: Failure cases for MM-Prompt